

Efficient discrimination schemes for unextendible product bases with strong quantum nonlocality

Qiqi Feng,¹ Huaqi Zhou,^{1,*} and Limin Gao^{1,2,†}

¹*School of Mathematics and Science, Hebei GEO University, Shijiazhuang 052161, China*

²*Intelligent Sensor Network Engineering Research Center of Hebei Province, Hebei GEO University, Shijiazhuang 052161, China*

Entanglement is a central resource in quantum information science; therefore, it is important to design local discrimination protocols that minimize resource consumption. In this paper, we propose three entanglement-allocation schemes for the local discrimination of particular unextendible product bases (UPB) exhibiting strong quantum nonlocality in a $3 \otimes 3 \otimes 3$ system. By exploiting the structural features of these UPB and the operational advantages of maximally entangled states, we further extend our protocols to strongly nonlocal UPB in $d \otimes d \otimes d$ systems. In particular, we show that these UPB can be perfectly distinguished with only two maximally entangled states. Moreover, a resource-cost analysis indicates that our protocols, which avoid quantum teleportation whenever possible, can reduce the entanglement consumption. These results not only facilitate resource-efficient quantum information processing, but also provide further insight into the operational role of maximally entangled states.

I. INTRODUCTION

Quantum state discrimination is a fundamental problem in quantum information theory. Beyond its role in decoding and extracting quantum information, it also underlies a broad range of tasks, including quantum secret sharing, quantum data hiding, and secure quantum communication [1–9]. Accordingly, given a set of mutually orthogonal states, a key question is to identify which state has been prepared.

For any set of orthogonal quantum states in a multipartite system, perfect discrimination is always possible via global measurements [10]. However, under the operational restriction of local operations and classical communication (LOCC)-namely, when spatially separated parties perform only local measurements and coordinate using classical messages [10–14]-even orthogonal states may become locally indistinguishable [15–20].

In 1999, Bennett *et al.* [10] first revealed “quantum nonlocality without entanglement” by constructing a complete orthogonal product bases in a $3 \otimes 3$ system. Although these states are perfectly distinguishable by global measurements, they cannot be perfectly distinguished by LOCC. This phenomenon exposes intrinsic limitations of LOCC-based discrimination, motivates systematic investigations of local distinguishability, and has stimulated extensive work on entanglement-assisted local discrimination. Since then, substantial progress has been made [21–35].

More recently, Halder *et al.* [34] introduced the notion of *strong quantum nonlocality*. Unextendible product bases (UPB) with strong quantum nonlocality form an important class of orthogonal product sets that are locally irreducible across every bipartition and, moreover, have the property that their orthogonal complements contain no product states [11, 36–39]. It is well known that suitable entanglement resources can regulate the local distinguishability of orthogonal sets [22, 39–44]. Consequently, optimizing the use of low-dimensional entanglement has become an active direction [39, 43–45]. In particular, Cohen [43] identified UPB that become LOCC-distinguishable with the aid of medium-dimensional maximally entangled states. Later, Zhang *et al.* [44] showed that multiple copies of $2 \otimes 2$ maximally entangled states (EPR pairs) can replace higher-dimensional entanglement, thereby reducing experimental complexity.

Entanglement is an exceptionally valuable quantum resource [46–49]. In practice, low-dimensional entangled states are appealing due to their relative ease of generation and control. Incorporating them into discrimination protocols can reduce both the entanglement cost and the operational overhead [50, 51]. Therefore, it is of considerable interest to develop efficient LOCC discrimination schemes relying only on low-dimensional entanglement.

In this work, we further investigate entanglement-assisted local discrimination of UPB. We first review preliminaries and definitions. We then consider a known strongly nonlocal UPB in a $3 \otimes 3 \otimes 3$ system [37] and propose two classes of LOCC protocols: one class uses teleportation, while the other avoids teleportation by optimizing the allocation of low-dimensional entanglement and coordinating multipartite local measurements. Building on these ideas, we generalize the schemes to $d \otimes d \otimes d$ systems, compare resource costs, and discuss the trade-offs among different protocols. We conclude with a brief summary.

*Electronic address: zhouchuaqilc@163.com

†Electronic address: gaoliminabc@163.com

II. PRELIMINARIES

In this section, we introduce basic concepts and notation used throughout the paper.

Definition 1 [11]. An unextendible product bases (UPB) is a set of pairwise orthogonal product states $\{\otimes_{j=1}^m |\psi\rangle_j^i\}_{i=1}^n$ spanning a proper subspace of $\otimes_{j=1}^m \mathbb{C}^{d_j}$ (i.e., $n < \prod_{j=1}^m d_j$). Moreover, the orthogonal complement of this subspace contains no product state.

Equivalently, a UPB cannot be extended by adding any additional product state while preserving mutual orthogonality. Consequently, its complementary subspace is necessarily entangled.

Definition 2 [34]. A set of orthogonal product states $\{\otimes_{j=1}^m |\psi\rangle_j^i\}_{i=1}^n$ on $\otimes_{j=1}^m \mathbb{C}^{d_j}$ is said to be *strongly nonlocal* if, for every bipartition, no nontrivial orthogonality-preserving local measurement can distinguish one or more states from the set.

Definition 3 [22]. In local state discrimination, an *entanglement resource configuration* specifies the type of entanglement resource, the average number of copies consumed, and the parties that share these resources.

In what follows, a resource configuration is denoted by $\{(N, |\phi^+(d)\rangle_{P_1 P_2}); (M, |\phi^+(d)\rangle_{P_2 P_3})\}$, where N and M are the average numbers of consumed resources, and $|\phi^+(d)\rangle = \frac{1}{\sqrt{d}} \sum_{i=0}^{d-1} |ii\rangle$ is a maximally entangled state. The subscripts specify which parties share the resource.

Definition 4. For any real number x , let $\lfloor x \rfloor$ and $\lceil x \rceil$ denote the floor and ceiling functions, respectively; that is, $\lfloor x \rfloor$ is the greatest integer not exceeding x , and $\lceil x \rceil$ is the smallest integer not less than x .

Based on these definitions, we design local discrimination protocols for UPB in $d \otimes d \otimes d$ systems under various resource-allocation scenarios, and we quantify the corresponding entanglement consumption for each protocol.

III. ENTANGLEMENT-ASSISTED DISCRIMINATION IN THE $3 \otimes 3 \otimes 3$ SYSTEM

We consider the following strongly nonlocal UPB in a $3 \otimes 3 \otimes 3$ system [37]:

$$\begin{aligned} \mathcal{A}_1 &:= \{|\xi_j\rangle_A |0\rangle_B |\eta_i\rangle_C \mid (i, j) \in \mathbb{Z}_2 \times \mathbb{Z}_2 \setminus \{(0, 0)\}\}, \\ \mathcal{A}_2 &:= \{|\xi_j\rangle_A |\eta_i\rangle_B |2\rangle_C \mid (i, j) \in \mathbb{Z}_2 \times \mathbb{Z}_2 \setminus \{(0, 0)\}\}, \\ \mathcal{A}_3 &:= \{|2\rangle_A |\xi_j\rangle_B |\eta_i\rangle_C \mid (i, j) \in \mathbb{Z}_2 \times \mathbb{Z}_2 \setminus \{(0, 0)\}\}, \\ \mathcal{B}_1 &:= \{|\eta_i\rangle_A |2\rangle_B |\xi_j\rangle_C \mid (i, j) \in \mathbb{Z}_2 \times \mathbb{Z}_2 \setminus \{(0, 0)\}\}, \\ \mathcal{B}_2 &:= \{|\eta_i\rangle_A |\xi_j\rangle_B |0\rangle_C \mid (i, j) \in \mathbb{Z}_2 \times \mathbb{Z}_2 \setminus \{(0, 0)\}\}, \\ \mathcal{B}_3 &:= \{|0\rangle_A |\eta_i\rangle_B |\xi_j\rangle_C \mid (i, j) \in \mathbb{Z}_2 \times \mathbb{Z}_2 \setminus \{(0, 0)\}\}, \\ |S\rangle &= \left(\sum_{i=0}^2 |i\rangle \right)_A \left(\sum_{j=0}^2 |j\rangle \right)_B \left(\sum_{k=0}^2 |k\rangle \right)_C. \end{aligned} \tag{1}$$

Here $|\eta_i\rangle = |0\rangle + (-1)^i |1\rangle$ and $|\xi_j\rangle = |1\rangle + (-1)^j |2\rangle$ for $i, j \in \mathbb{Z}_2$. The UPB $\bigcup_{i=1}^3 (\mathcal{A}_i \cup \mathcal{B}_i) \cup \{|S\rangle\}$ cannot be perfectly distinguished by LOCC. Since it is a lowest-dimensional example of strong nonlocality without entanglement in the $3 \otimes 3 \otimes 3$ setting, an important question is the following: *What minimum entanglement is required to enable perfect local discrimination of such a highly constrained UPB?* To address this, we propose three entanglement-assisted discrimination schemes. By exploiting the block structure of the set, our protocols reduce entanglement consumption compared with the naive approach of teleporting the entire multipartite state to a single party.

Theorem 1. The entanglement resource configuration $\{(1, |\phi^+(2)\rangle_{AB}); (1, |\phi^+(3)\rangle_{BC})\}$ is sufficient for perfectly distinguishing the UPB (1) by LOCC.

Proof. Let the system be shared by Alice, Bob, and Charlie. Using the maximally entangled resource $|\phi^+(3)\rangle$, Charlie first teleports subsystem C to Bob. Let \tilde{B} denote Bob's enlarged system comprising his original subsystem B and the teleported subsystem C . Alice and Bob additionally share an EPR state $|\phi^+(2)\rangle_{ab} = |00\rangle_{ab} + |11\rangle_{ab}$. The initial joint state can be written as

$$|\psi\rangle_{A\tilde{B}} \otimes |\phi^+(2)\rangle_{ab}. \tag{2}$$

For brevity, we write $|ij\rangle = |i\rangle \otimes |j\rangle = |3i + j\rangle$. Since each subset \mathcal{A}_i and \mathcal{B}_i ($i = 1, 2, 3$) is LOCC-distinguishable once identified, it suffices to distinguish among these subsets.

Step 1. Alice performs the measurement

$$\mathcal{M}_1 \equiv \{M_{11} := P[|0\rangle, |1\rangle)_A; |0\rangle_a] + P[|2\rangle_A; |1\rangle_a], M_{12} := I - M_{11}\}.$$

Here $P[(|0\rangle, |1\rangle)_A; |0\rangle_a] := (|0\rangle\langle 0| + |1\rangle\langle 1|)_A \otimes (|0\rangle\langle 0|)_a$, and analogous notation applies throughout.

Conditioned on outcome M_{11} (cf. Fig. 1), the post-measurement states become

$$\begin{aligned}\mathcal{A}_1 &\rightarrow \{(|1\rangle_A|00\rangle_{ab} + (-1)^j|2\rangle_A|11\rangle_{ab})|0\circ\eta_i\rangle_{\tilde{B}}\}, \\ \mathcal{A}_2 &\rightarrow \{(|1\rangle_A|00\rangle_{ab} + (-1)^j|2\rangle_A|11\rangle_{ab})|\eta_i\circ 2\rangle_{\tilde{B}}\}, \\ \mathcal{A}_3 &\rightarrow \{|2\rangle_A|\xi_j\circ\eta_i\rangle_{\tilde{B}}|11\rangle_{ab}\}, \\ \mathcal{B}_1 &\rightarrow \{|\eta_i\rangle_A|2\circ\xi_j\rangle_{\tilde{B}}|00\rangle_{ab}\}, \\ \mathcal{B}_2 &\rightarrow \{|\eta_i\rangle_A|\xi_j\circ 0\rangle_{\tilde{B}}|00\rangle_{ab}\}, \\ \mathcal{B}_3 &\rightarrow \{|0\rangle_A|\eta_i\circ\xi_j\rangle_{\tilde{B}}|00\rangle_{ab}\}, \\ |S\rangle &\rightarrow ((|0\rangle + |1\rangle)_A|00\rangle_{ab} + |2\rangle_A|11\rangle_{ab})|\gamma\circ\gamma\rangle_{\tilde{B}},\end{aligned}$$

where $|\gamma\rangle = |0\rangle + |1\rangle + |2\rangle$. Hereafter, the symbol “ \circ ” denotes tensor concatenation of subsystems: for states $|\psi_1\rangle_B$ and $|\psi_2\rangle_C$, $|\psi_1\circ\psi_2\rangle_{\tilde{B}} = |\psi_1\rangle_B \otimes |\psi_2\rangle_C$. In particular, $|(0, \dots, d_B - 1) \circ (0, \dots, d_C - 1)\rangle_{\tilde{B}}$ denotes the computational basis of \tilde{B} ordered lexicographically.

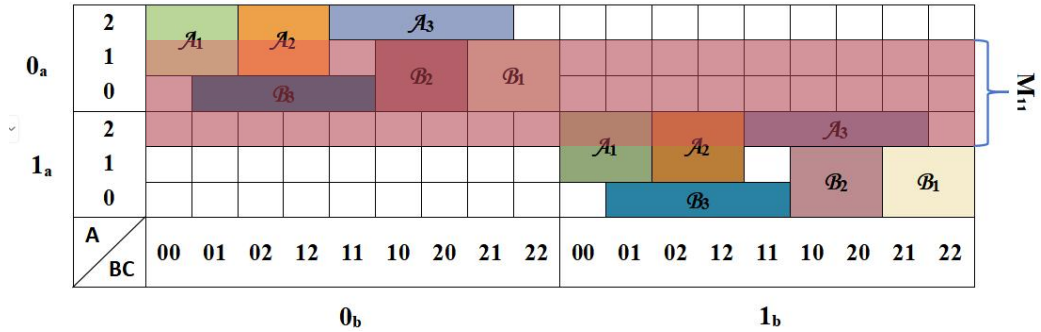


FIG. 1: With the shared EPR state $|\phi^+(2)\rangle_{ab}$, the state in Eq. (2) can be represented on a $2d_A \times 2d_B d_C$ grid. The lavender-shaded region indicates the support of M_{11} .

Step 2. Bob performs

$$\begin{aligned}\mathcal{M}_2 &\equiv \{ M_{21} := P[|(1, 2) \circ (0, 1)\rangle_{\tilde{B}}; |1\rangle_b], \\ M_{22} &:= P[|2 \circ (1, 2)\rangle_{\tilde{B}}; |0\rangle_b], \\ M_{23} &:= P[|(1, 2) \circ 0\rangle_{\tilde{B}}; |0\rangle_b], \\ M_{24} &:= I - M_{21} - M_{22} - M_{23} \}.\end{aligned}$$

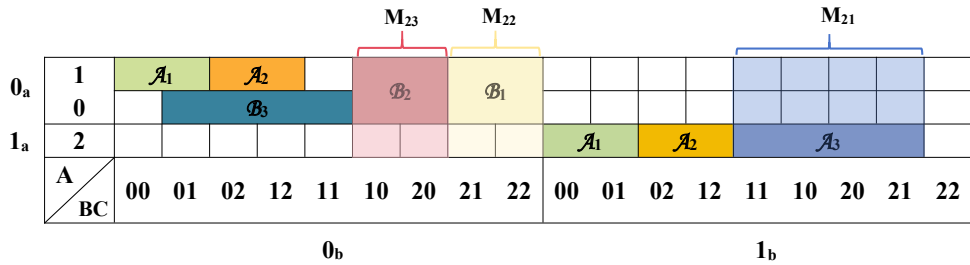


FIG. 2: The lightly shaded regions represent the measurement outcomes in the M_{21} , M_{22} , and M_{23} directions for Bob, respectively.

The measurement outcomes corresponding to the operators M_{21} , M_{22} , M_{23} (see Fig. 2) are

$$\begin{aligned}M_{21} &\Rightarrow \mathcal{A}_3 \text{ and } |S\rangle \rightarrow |2\rangle_A|11\rangle_{ab}(|10\rangle + |11\rangle + |20\rangle + |21\rangle)_{\tilde{B}}, \\ M_{22} &\Rightarrow \mathcal{B}_1 \text{ and } |S\rangle \rightarrow (|0\rangle + |1\rangle)_A|00\rangle_{ab}(|21\rangle + |22\rangle)_{\tilde{B}}, \\ M_{23} &\Rightarrow \mathcal{B}_2 \text{ and } |S\rangle \rightarrow (|0\rangle + |1\rangle)_A|00\rangle_{ab}(|10\rangle + |20\rangle)_{\tilde{B}},\end{aligned}$$

respectively. Clearly, these can be perfectly distinguished. If M_{24} clicks, the states falls into one of these remaining subsets \mathcal{A}_1 , \mathcal{A}_2 , \mathcal{B}_3 and state $|S\rangle \rightarrow (|0\rangle + |1\rangle)_A |00\rangle_{ab} (|00\rangle + |01\rangle + |02\rangle + |11\rangle + |12\rangle)_{\tilde{B}} + |2\rangle_A |11\rangle_{ab} (|00\rangle + |01\rangle + |02\rangle + |12\rangle + |22\rangle)_{\tilde{B}}$.
 Step 2. Alice performs

Step 3. Alice performs

$$\mathcal{M}_3 \equiv \{ M_{31} := P[|0\rangle_A; |0\rangle_a], M_{32} := I - M_{31} \}.$$

As shown in Fig. 3, if M_{31} clicks, the resulting subsets are \mathcal{B}_3 and $\{|S\rangle\} \rightarrow \{|0\rangle_A|00\rangle_{ab}(|00\rangle + |01\rangle + |02\rangle + |11\rangle + |12\rangle)\tilde{B}\}$, which are locally distinguishable. Otherwise, the given subset is one of the following \mathcal{A}_1 , \mathcal{A}_2 and $\{|S\rangle\} \rightarrow \{|1\rangle_A|00\rangle_{ab}(|00\rangle + |01\rangle + |02\rangle + |11\rangle + |12\rangle)\tilde{B} + |2\rangle_A|11\rangle_{ab}(|00\rangle + |01\rangle + |02\rangle + |12\rangle + |22\rangle)\tilde{B}\}$.

FIG. 3: The measurement result for direction M_{31} in Alice's subsystem corresponds to the pale green region.

Step 4. Bob performs

$$\mathcal{M}_4 \equiv \{ M_{41} := P[(|00\rangle, |01\rangle)_{\tilde{B}}; (|0\rangle, |1\rangle)_b], M_{42} := I - M_{41} \}.$$

If M_{41} clicks, the resulting subsets are \mathcal{A}_1 and $\{|S\rangle\} \rightarrow \{|1\rangle_A|00\rangle_{ab} + |2\rangle_A|11\rangle_{ab}\}(|00\rangle + |01\rangle)_{\tilde{B}}$. Otherwise, the subsets are \mathcal{A}_2 and $\{|S\rangle\} \rightarrow \{|1\rangle_A|00\rangle_{ab}(|02\rangle + |11\rangle + |12\rangle)_{\tilde{B}} + |2\rangle_A|11\rangle_{ab}(|02\rangle + |12\rangle + |22\rangle)_{\tilde{B}}\}$. Evidently, these subsets are LOCC distinguishable.

If M_{12} clicks in the step 1, then also a similar discrimination protocol follows.

The final state $|S\rangle$ in above process will not affect the application of the discrimination scheme because $|S\rangle$ is a stopper state in UPB (1) and can be encoded useless information. We also find that the union of the single subset distinguished and the corresponding $|S\rangle$ can always be locally discriminated after performing the orthogonality-preserving projection measurement. So, we will no longer discuss the state $|S\rangle$ in the following protocols.

Theorem 2. The resource configuration $\{(1, |\phi^+(2)\rangle_{AB}); (1, |\phi^+(2)\rangle_{BC})\}$ is sufficient for perfectly distinguishing the UPB (1) by LOCC.

Proof. Assume that Alice–Bob and Alice–Charlie each share an EPR state. Bob performs

$$\mathcal{M}_1 \equiv \{M_{11} := P[|0\rangle_B; |0\rangle_{b_1}] + P[|1\rangle, |2\rangle)_B; |1\rangle_{b_1}], M_{12} := I - M_{11}\},$$

and Charlie performs

$$\mathcal{M}_2 \equiv \{M_{21} := P[(|0\rangle, |1\rangle)_C; |0\rangle_{c_1}] + P[|2\rangle_C; |1\rangle_{c_1}], M_{22} := I - M_{21}\}.$$

Conditioned on the outcomes M_{11} and M_{21} , the resulting post-measurement states are

$$\begin{aligned}
\mathcal{A}_1 &\rightarrow \{ |\xi_j\rangle_A |0\rangle_B |\eta_i\rangle_C |00\rangle_{a_1b_1} |00\rangle_{a_2c_1} \}, \\
\mathcal{A}_2 &\rightarrow \{ |\xi_j\rangle_A (|0\rangle_B |00\rangle_{a_1b_1} + (-1)^i |1\rangle_B |11\rangle_{a_1b_1}) |2\rangle_C |11\rangle_{a_2c_1} \}, \\
\mathcal{A}_3 &\rightarrow \{ |2\rangle_A |\xi_j\rangle_B |11\rangle_{a_1b_1} |\eta_i\rangle_C |00\rangle_{a_2c_1} \}, \\
\mathcal{B}_1 &\rightarrow \{ |\eta_i\rangle_A |2\rangle_B |11\rangle_{a_1b_1} (|1\rangle_C |00\rangle_{a_2c_1} + (-1)^j |2\rangle_C |11\rangle_{a_2c_1}) \}, \\
\mathcal{B}_2 &\rightarrow \{ |\eta_i\rangle_A |\xi_j\rangle_B |11\rangle_{a_1b_1} |0\rangle_C |00\rangle_{a_2c_1} \}, \\
\mathcal{B}_3 &\rightarrow \{ |0\rangle_A (|0\rangle_B |00\rangle_{a_1b_1} + (-1)^i |1\rangle_B |11\rangle_{a_1b_1}) (|1\rangle_C |00\rangle_{a_2c_1} + (-1)^j |2\rangle_C |11\rangle_{a_2c_1}) \}.
\end{aligned}$$

Step 2. Alice performs the measurement

$$\mathcal{M}_3 = \{M_{31} := P[(|1\rangle, |2\rangle)_A; |0\rangle_{a_1}; |0\rangle_{a_2}], M_{32} := P[|2\rangle_A; |1\rangle_{a_1}; |0\rangle_{a_2}], M_{33} := I - M_{31} - M_{32}\}.$$

The measurement outcomes corresponding to M_{31} and M_{32} are \mathcal{A}_1 and \mathcal{A}_3 , respectively. These states can be locally distinguished by Bob's measurement. Other, operation M_{33} leaves \mathcal{A}_2 and \mathcal{B}_i with $i = 1, 2, 3$.

Step 3. Charlie performs the measurement

$$\mathcal{M}_4 \equiv \{ M_{41} := P[|0\rangle_C; |0\rangle_{c_1}], M_{42} := I - M_{41} \}.$$

If M_{41} clicks, we obtain the subset \mathcal{B}_2 which is perfectly LOCC distinguishable.

Step 4. Bob performs the measurement

$$\mathcal{M}_5 \equiv \{ M_{51} := P[|2\rangle_B; |1\rangle_{b_1}], M_{52} := I - M_{51} \}.$$

Suppose M_{51} clicks, the subset is \mathcal{B}_1 which is perfectly LOCC distinguishable. M_{52} is a projection operator acting in Bob's party, it leaves \mathcal{A}_2 and \mathcal{B}_3 .

Step 5. Alice performs the measurement

$$\mathcal{M}_6 \equiv \{ M_{61} := P[|1\rangle, |2\rangle)_A; (|0\rangle, |1\rangle)_{a_1}; |1\rangle_{a_2}], M_{62} := I - M_{61} \}.$$

If M_{61} clicks, the corresponding subset is \mathcal{A}_2 . Otherwise, the subset is \mathcal{B}_3 . These are perfectly LOCC distinguishable.

In addition, if other operators click in the step 1, we can find similar discrimination schemes. \square

Theorem 3. The resource configuration $\{(1, |\phi^+(3)\rangle_{ABC})\}$ is sufficient for perfectly distinguishing the UPB (1), where $|\phi^+(3)\rangle_{ABC} = \frac{1}{\sqrt{3}} \sum_{i=0}^2 |iii\rangle_{ABC}$.

Proof. To locally discriminate the set (1), let Alice, Bob and Charlie share a maximally entangled state $|\phi^+(3)\rangle_{ABC}$. Now, we only needs to locally distinguish these subsets \mathcal{A}_i and \mathcal{B}_i for $i = 1, 2, 3$.

Step 1. Alice performs a measurement

$$\mathcal{M}_1 \equiv \{ M_{11} := P[|0\rangle_A; |0\rangle_a] + P[|1\rangle, |2\rangle)_A; (|1\rangle, |2\rangle)_a], M_{12} := I - M_{11} \}.$$

Charlie performs a measurement

$$\mathcal{M}_2 \equiv \{ M_{21} := P[|0\rangle, |1\rangle)_C; |1\rangle_a] + P[|2\rangle_C; |2\rangle_c] + P[I_C; |0\rangle_c], M_{22} := I - M_{21} \}.$$

The quantum states corresponding to the measurement outcomes M_1 and M_2 are as follows.

$$\begin{aligned} \mathcal{A}_1 &\rightarrow \{ |\xi_j\rangle_A |0\rangle_B |\eta_i\rangle_C |111\rangle_{abc} \}, \\ \mathcal{A}_2 &\rightarrow \{ |\xi_j\rangle_A |\eta_i\rangle_B |2\rangle_C |222\rangle_{abc} \}, \\ \mathcal{A}_3 &\rightarrow \{ |2\rangle_A |\xi_j\rangle_B |\eta_i\rangle_C |111\rangle_{abc} \}, \\ \mathcal{B}_1 &\rightarrow \{ |0\rangle_A |2\rangle_B |\xi_j\rangle_C |000\rangle_{abc} + (-1)^i |1\rangle_A |2\rangle_B (|1\rangle_C |111\rangle_{abc} + (-1)^j |2\rangle_C |222\rangle_{abc}) \}, \\ \mathcal{B}_2 &\rightarrow \{ (|0\rangle_A |000\rangle_{abc} + (-1)^i |1\rangle_A |111\rangle_{abc}) |\xi_j\rangle_B |0\rangle_C \}, \\ \mathcal{B}_3 &\rightarrow \{ |0\rangle_A |\eta_i\rangle_B |\xi_j\rangle_C |000\rangle_{abc} \}. \end{aligned}$$

Step 2. Bob performs the measurement

$$\mathcal{M}_3 \equiv \{ M_{31} := P[|0\rangle_B; |1\rangle_b], M_{32} := P[|0\rangle, |1\rangle)_B; |2\rangle_b], M_{33} := I - M_{31} - M_{32} \}.$$

The measurement outcomes corresponding to M_{31} and M_{32} are \mathcal{A}_1 and \mathcal{A}_2 , respectively. For operator M_{33} , there are several of the subsets \mathcal{A}_3 and \mathcal{B}_i with $i = 1, 2, 3$.

Step 3. Alice performs the measurement

$$M_4 \equiv \{ \mathcal{M}_{41} := P[|2\rangle_A; |1\rangle_a], M_{42} := I - M_{41} \}.$$

If M_{41} clicks, the subset is \mathcal{A}_3 . Otherwise, the given state is belonging to one of the remaining subsets \mathcal{B}_1 , \mathcal{B}_2 and \mathcal{B}_3 .

Step 4. Charlie performs the measurement

$$\mathcal{M}_5 \equiv \{ M_{51} := P[|0\rangle_C; (|0\rangle, |1\rangle)_c], M_{52} := I - M_{51} \}.$$

The outcomes acquired from implementing the measurement M_{51} is \mathcal{B}_2 . Otherwise, the state belongs to one of the subsets \mathcal{B}_1 and \mathcal{B}_3 .

Step 5. Bob performs the measurement

$$\mathcal{M}_6 \equiv \{ M_{61} := P[|0\rangle, |1\rangle)_B; |0\rangle_b], M_{62} := I - M_{61} \}.$$

The outcomes acquired from implementing the measurement M_{61} is \mathcal{B}_3 . Otherwise, the state is an element of the subset \mathcal{B}_1 .

If another operator clicks in the step 1, we can obtain a similar entanglement-assisted discrimination protocol to distinguish set (1). \square

Resource comparison. Theorem 1 uses one teleportation round and consumes $(1 + \log_2 3)$ ebits in total. Theorem 2 avoids teleportation and achieves the same task using two EPR pairs, i.e., 2 ebits. Theorem 3 also avoids teleportation and uses a single tripartite maximally entangled state. In contrast, a strategy based solely on teleportation of full subsystems would require at least $2 \log_2 3$ ebits. Overall, the proposed schemes outperform naive teleportation in entanglement cost. Moreover, Theorem 2 indicates that two EPR pairs can play a role operationally comparable to $|\phi^+(3)\rangle_{ABC}$ for this discrimination task, while EPR pairs are typically more accessible experimentally. Consequently, the choice among Theorems 2 and 3 can be guided by implementation constraints. We next generalize these results to $d \otimes d \otimes d$ systems with $d \geq 3$.

IV. QUANTUM STATE DISCRIMINATION IN $d \otimes d \otimes d$

We recall the construction of strongly nonlocal UPB in $d \otimes d \otimes d$ systems ($d \geq 3$) from Ref. [37].

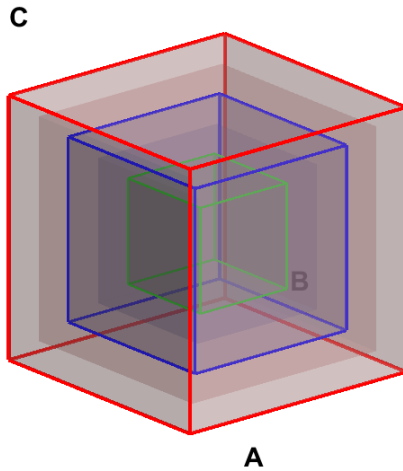


FIG. 4: Layered cubic structure of the set in Eq. (3) within a $d \otimes d \otimes d$ tripartite system.

$$\begin{aligned}
 \mathcal{A}_1^{(d,d-2k)} &:= \left\{ \left| \xi_j^{(d-2k)} \right\rangle_A |k\rangle_B \left| \eta_i^{(d-2k)} \right\rangle_C \mid (i, j) \in \mathbb{Z}_{d-1-2k} \times \mathbb{Z}_{d-1-2k} \setminus \{(0, 0)\} \right\}, \\
 \mathcal{A}_2^{(d,d-2k)} &:= \left\{ \left| \xi_j^{(d-2k)} \right\rangle_A \left| \eta_i^{(d-2k)} \right\rangle_B |d-1-k\rangle_C \mid (i, j) \in \mathbb{Z}_{d-1-2k} \times \mathbb{Z}_{d-1-2k} \setminus \{(0, 0)\} \right\}, \\
 \mathcal{A}_3^{(d,d-2k)} &:= \left\{ |d-1-k\rangle_A \left| \xi_j^{(d-2k)} \right\rangle_B \left| \eta_i^{(d-2k)} \right\rangle_C \mid (i, j) \in \mathbb{Z}_{d-1-2k} \times \mathbb{Z}_{d-1-2k} \setminus \{(0, 0)\} \right\}, \\
 \mathcal{B}_1^{(d,d-2k)} &:= \left\{ \left| \eta_i^{(d-2k)} \right\rangle_A |d-1-k\rangle_B \left| \xi_j^{(d-2k)} \right\rangle_C \mid (i, j) \in \mathbb{Z}_{d-1-2k} \times \mathbb{Z}_{d-1-2k} \setminus \{(0, 0)\} \right\}, \\
 \mathcal{B}_2^{(d,d-2k)} &:= \left\{ \left| \eta_i^{(d-2k)} \right\rangle_A \left| \xi_j^{(d-2k)} \right\rangle_B |k\rangle_C \mid (i, j) \in \mathbb{Z}_{d-1-2k} \times \mathbb{Z}_{d-1-2k} \setminus \{(0, 0)\} \right\}, \\
 \mathcal{B}_3^{(d,d-2k)} &:= \left\{ |k\rangle_A \left| \eta_i^{(d-2k)} \right\rangle_B \left| \xi_j^{(d-2k)} \right\rangle_C \mid (i, j) \in \mathbb{Z}_{d-1-2k} \times \mathbb{Z}_{d-1-2k} \setminus \{(0, 0)\} \right\}, \\
 |S_d\rangle &:= \left(\sum_{i=0}^{d-1} |i\rangle \right)_A \left(\sum_{j=0}^{d-1} |j\rangle \right)_B \left(\sum_{k=0}^{d-1} |k\rangle \right)_C,
 \end{aligned} \tag{3}$$

where $|\eta_i^{(d-2k)}\rangle = \sum_{t=k}^{d-2-k} w_{d-1-2k}^{i(t-k)} |t\rangle$ and $|\xi_j^{(d-2k)}\rangle = \sum_{t=k}^{d-2-k} w_{d-1-2k}^{j(t-k)} |t+1\rangle$ for $i, j \in \mathbb{Z}_{d-1-2k}$ and $k = 0, \dots, \lceil \frac{d}{2} \rceil - 2$. Let $\mathcal{A}^{(d,0)} = \{|\phi_r\rangle_A |\phi_s\rangle_B |\phi_t\rangle_C \mid (r, s, t) \in \mathbb{Z}_2^3 \setminus \{(0, 0, 0)\}\}$, where $|\phi_i\rangle = \left| \frac{d-2}{2} \right\rangle + (-1)^i \left| \frac{d}{2} \right\rangle$ for $i \in \mathbb{Z}_2$ (defined only when

d is even). These sets form a strongly nonlocal UPB:

$$\mathcal{U}_d = \begin{cases} \bigcup_{i=1}^3 \bigcup_{k=0}^{\frac{d-3}{2}} \left(\mathcal{A}_i^{(d,d-2k)} \cup \mathcal{B}_i^{(d,d-2k)} \right) \cup \{|S_d\rangle\}, & d \text{ odd}, \\ \bigcup_{i=1}^3 \bigcup_{k=0}^{\frac{d-4}{2}} \left(\mathcal{A}_i^{(d,d-2k)} \cup \mathcal{B}_i^{(d,d-2k)} \right) \cup \{|S_d\rangle\} \cup \mathcal{A}^{(d,0)}, & d \text{ even}. \end{cases} \quad (4)$$

Geometrically, the set \mathcal{U}_d can be visualized as occupying a three-dimensional $d \times d \times d$ lattice with a “Rubik’s cube-like” layered structure: it consists of nested concentric shells indexed by k . As illustrated in Fig. 4, $k = 0$ corresponds to the outermost layer and $k = 1$ to the next layer, and so forth. Using this structure, we propose three discrimination protocols.

Theorem 4. In $d \otimes d \otimes d$, the strongly nonlocal UPB \mathcal{U}_d in Eq. (4) can be perfectly distinguished by LOCC using the resource configuration $\{(1, |\phi^+(\lceil \frac{d}{2} \rceil)\rangle_{AB}); (1, |\phi^+(\lceil \frac{d}{2} \rceil)\rangle_{BC})\}$.

Proof. Since each subset provided by Eq. (3) and subset $\mathcal{A}^{(d,0)}$ are locally distinguishable, we only need to distinguish these subsets. There are three key steps. First, we execute once quantum teleportation with a maximally entangled state $|\phi^+(d)\rangle_{BC} = \frac{1}{\sqrt{d}} \sum_{i=1}^d |ii\rangle_{BC}$ such that the quantum state is jointly owned by Alice and Bob and denoted as $|\psi\rangle_{A\tilde{B}}$. Then, Alice and Bob share the maximally entangled state $|\phi^+(\lceil \frac{d}{2} \rceil)\rangle_{ab}$ and obtain the initial state $|\psi\rangle_{A\tilde{B}} \otimes |\phi^+(\lceil \frac{d}{2} \rceil)\rangle_{ab}$. Finally, a deterministic local discrimination protocol is designed based on this initial state. The detailed operational procedure, construction of measurement operators, and derivation of state evolution for the discrimination scheme are provided in Appendix A. \square

With the results established above, we consume a total of $\log_2 d + \log_2(\lceil \frac{d}{2} \rceil)$ ebits entanglement. The local dimension of $|\phi^+(\lceil \frac{d}{2} \rceil)\rangle$ is relatively high. Next, we provide a new resource configuration by replacing high-dimensional maximally entangled states $|\phi^+(\lceil \frac{d}{2} \rceil)\rangle$ with multiple copies of EPR states.

Theorem 5. In $d \otimes d \otimes d$, the set \mathcal{U}_d in Eq. (4) can be perfectly distinguished by LOCC using one teleportation round and $\lceil \frac{d}{2} - 1 \rceil$ copies of $2 \otimes 2$ maximally entangled states.

Proof. To realize the local discrimination of the quantum states in Eq. (4), the specific discrimination strategy is presented as follows. By leveraging the entangled resource $|\phi^+(d)\rangle_{BC}$, Charlie first performs quantum teleportation to transfer the quantum state of subsystem C to Bob, and the composite system is denoted as \tilde{B} .

To begin with, in the first round of the discrimination protocol, Alice and Bob share the first EPR state $|\phi^+(2)\rangle_{a_0b_0} = \frac{1}{\sqrt{2}} (|00\rangle + |11\rangle)_{a_0b_0}$. By using the same method as the protocol in Theorem 1, we can distinguish the subsets $\mathcal{A}_3^{(d,d)}, \mathcal{B}_1^{(d,d)}, \mathcal{B}_2^{(d,d)}, \mathcal{B}_3^{(d,d)}, \mathcal{A}_1^{(d,d)}$, and $\mathcal{A}_2^{(d,d)}$ of the outermost layer (i.e., $k = 0$) of set \mathcal{U}_d (4). After completing the first round of measurements, for the remaining quantum states, we further shared the second EPR state ($|\phi^+(2)\rangle_{a_1b_1} = \frac{1}{\sqrt{2}} (|00\rangle + |11\rangle)_{a_1b_1}$) between the Alice and Bob. Similarly, the subsets $\mathcal{A}_3^{(d,d-2)}, \mathcal{B}_1^{(d,d-2)}, \mathcal{B}_2^{(d,d-2)}, \mathcal{B}_3^{(d,d-2)}, \mathcal{A}_1^{(d,d-2)}$ and $\mathcal{A}_2^{(d,d-2)}$ can be distinguished individually. Repeat the above operations until we introduce the $\lceil \frac{d}{2} - 1 \rceil$ th EPR state. Details are provided in Appendix B. \square

The entanglement resources consumed in this protocol consist of two parts. One part, the process for quantum teleportation consumes $\log_2 d$ ebits entanglement resource. Other part, we introduce the EPR state in $\lceil \frac{d}{2} - 1 \rceil$ stages. The entanglement resource is consumed a total of $e = \sum_{m=0}^{\lceil d/2-2 \rceil} \frac{(d-2m)^3 - 8\lceil \frac{d}{2} - 1 - m \rceil}{d^3 - 8\lceil \frac{d}{2} - 1 \rceil}$ ebits (Refer to Appendix B). Thus, perfect discrimination of this set requires merely $\log_2 d + e$ ebits of entangled resources. As shown in Fig. 5, in terms of entanglement resource consumption, Theorems 4 and 5 consume the same amount of entanglement when $d = 4$. Theorem 5 uses fewer resources when $2 < d/2 \leq 12$, while Theorem 4 becomes more efficient in resource consumption when $d/2 > 12$. We find that the effect of $\lceil \frac{d}{2} - 1 \rceil$ copies of EPR states are equivalent to $|\phi^+(\lceil \frac{d}{2} \rceil)\rangle_{ab}$. We can replace a $|\phi^+(\lceil \frac{d}{2} \rceil)\rangle_{ab}$ with multiple EPR states. From the perspective of experimental implementation, the multiple EPR states employed in Theorem 5 are easier to prepare compared with the single high-dimensional entangled state required in Theorem 4, making Theorem 5 simpler in experimental operation and lower in implementation difficulty. So, we can choose the scheme of Theorem 5 when the local dimension d is small.

Theorem 6. In $d \otimes d \otimes d$, the resource configuration $\{(1, |\phi^+(\lceil \frac{d}{2} \rceil)\rangle_{AB}); (1, |\phi^+(\lceil \frac{d}{2} \rceil)\rangle_{AC})\}$ is sufficient for perfect LOCC discrimination of \mathcal{U}_d in Eq. (4).

Proof. To achieve local distinguishability of the sets in Eq. (4), let Alice share $|\phi^+(\lceil \frac{d}{2} \rceil)\rangle = \frac{1}{\sqrt{\lceil d/2 \rceil}} \sum_{i=0}^{\lceil d/2 \rceil - 1} |ii\rangle$ entangled states with Bob and Charlie, respectively. Then, the associated initial state is $|\psi\rangle_{ABC} \otimes |\lceil \frac{d}{2} \rceil\rangle_{a_1b_1} \otimes |\lceil \frac{d}{2} \rceil\rangle_{a_2c_1}$. Our discrimination protocol consists of four steps. First, local measurement is performed at Alice to effectively distinguish the subsets $\mathcal{A}_1^{(d,d-2k)}$ and $\mathcal{A}_3^{(d,d-2k)}$. Second, we perform a measurement on party C and identify the corresponding subset $\mathcal{B}_2^{(d,d-2k)}$. Further, we perform a measurement in Bob’s party, the target subset $\mathcal{B}_1^{(d,d-2k)}$ is obtained. Finally, we distinguish the remaining subsets based on the parity of d . If d is odd, we only need to discriminate the subsets $\mathcal{A}_2^{(d,d-2k)}$ and $\mathcal{B}_3^{(d,d-2k)}$ by the local measurement on party A . If d is even, the three subsets $\mathcal{A}_2^{(d,d-2k)}, \mathcal{B}_3^{(d,d-2k)}$ and $\mathcal{A}^{(d,0)}$ are required to be confirmed. Details are given in Appendix C. \square

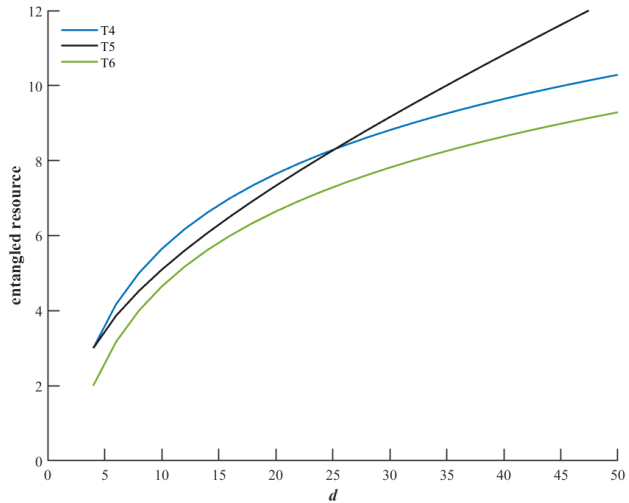


FIG. 5: T4, T5, and T6 are the curves of entanglement resource consumed by discrimination protocols in Theorems 4, 5, 6 corresponding to even dimension d , respectively.

In this protocol, we don't use quantum teleportation and only need two $|\phi^+(\lceil \frac{d}{2} \rceil)\rangle$. The total entangled resource consumed is $2\log_2(\lceil \frac{d}{2} \rceil)$ ebits, which is smaller than $\log_2 d + \log_2(\lceil \frac{d}{2} \rceil)$ of Theorem 4. Combining with the Fig. 5, we observe that the entanglement resources consumed by Theorem 4 and Theorem 5 are both higher than those of Theorem 6 when the dimension $d \geq 3$, indicating that Theorem 6 is more efficient. Both Theorem 4 and Theorem 5 rely on one round of quantum teleportation. Among these three distinguishable processes, the protocol without quantum teleportation performs better than with quantum teleportation.

V. CONCLUSION

We investigated entanglement-assisted LOCC discrimination protocols for the strongly nonlocal UPB introduced in Ref. [37] under different entanglement resources. For the $3 \otimes 3 \otimes 3$ case, we showed that deterministic perfect discrimination can be achieved using only two EPR pairs. This provides a partial answer to the open question raised in Ref. [44] concerning the existence of families of states that admit deterministic LOCC discrimination using only multiple copies of $2 \otimes 2$ maximally entangled states and without teleportation.

We further extended these schemes to $d \otimes d \otimes d$ systems and obtained Theorems 4–6. Compared with the approach in Ref. [37], which requires two teleportation rounds to discriminate \mathcal{U}_d , our Theorems 4 and 6 reduce the entanglement cost. Theorem 5 uses one teleportation round together with multiple EPR pairs. While its resource consumption can exceed that of Ref. [37] for large d , it may be more feasible experimentally and can reduce implementation complexity. Overall, teleportation-free schemes tend to be more entanglement-efficient, thereby enriching the study of UPB and further clarifying the operational role of maximally entangled states.

Acknowledgments

This work was supported by the National Natural Science Foundation of China under grant no. 12526564, the Natural Science Foundation of Hebei Province under grant no. A2025403008, and the Doctoral Science Start Foundation of Hebei GEO University of China under grant no. BQ2024075.

Appendix-wide notation and conventions. Throughout this appendix, Charlie teleports subsystem C to Bob (when required) so that Bob holds the composite system $\tilde{B} := B \otimes C$. We continue to use the concatenation symbol “ \circ ” to denote the tensor product across B and C , i.e., $|\psi_1 \circ \psi_2\rangle_{\tilde{B}} := |\psi_1\rangle_B \otimes |\psi_2\rangle_C$. For a register X , we write

$$P[(|i_1\rangle, \dots, |i_r\rangle)_X; |j\rangle_Y] := \left(\sum_{\ell=1}^r |i_\ell\rangle\langle i_\ell|_X \right) \otimes |j\rangle\langle j|_Y,$$

and analogous extensions (e.g. with a span on Y) are used in the same way as in the main text. As in the main text, we omit the explicit post-measurement form of the stopper state $|S_d\rangle$, since it can be treated without affecting orthogonality-preserving branches.

Appendix A: Proof of Theorem 4

Initial resources and state. Charlie and Bob share a maximally entangled state $|\phi^+(d)\rangle_{BC}$ and perform one round of quantum teleportation so that Bob receives C . Hence, the unknown state becomes $|\psi\rangle_{A\tilde{B}}$ with $\tilde{B} = BC$. In addition, Alice and Bob share one maximally entangled state

$$|\phi^+(\lceil d/2 \rceil)\rangle_{ab} = \frac{1}{\sqrt{\lceil d/2 \rceil}} \sum_{r=0}^{\lceil d/2 \rceil - 1} |rr\rangle_{ab}.$$

Therefore, the overall initial state for the discrimination stage is $|\psi\rangle_{A\tilde{B}} \otimes |\phi^+(\lceil d/2 \rceil)\rangle_{ab}$, where $|\psi\rangle_{A\tilde{B}}$ is any element of \mathcal{U}_d in Eq. (4).

Step 1 (Alice). Alice performs the POVM

$$\mathcal{M}_1 \equiv \{M_{11}, M_{12}, \dots, M_{1\lceil d/2 \rceil}\},$$

whose elements are

$$\begin{aligned} \mathcal{M}_1 \equiv & \left\{ M_{11} := P \left[\left(|0\rangle, |1\rangle, \dots, \left| \left\lfloor \frac{d}{2} \right\rfloor \right\rangle \right)_A ; |0\rangle_a \right] + P \left[\left| \left\lfloor \frac{d}{2} \right\rfloor + 1 \right\rangle_A ; |1\rangle_a \right] + \dots \right. \\ & + P \left[|d-2\rangle_A ; \left| \left\lfloor \frac{d}{2} \right\rfloor - 2 \right\rangle_a \right] + P \left[|d-1\rangle_A ; \left| \left\lfloor \frac{d}{2} \right\rfloor - 1 \right\rangle_a \right], \\ M_{12} := & P \left[\left(|0\rangle, |1\rangle, \dots, \left| \left\lfloor \frac{d}{2} \right\rfloor \right\rangle \right)_A ; |1\rangle_a \right] + P \left[\left| \left\lfloor \frac{d}{2} \right\rfloor + 1 \right\rangle_A ; |2\rangle_a \right] + \dots \\ & + P \left[|d-2\rangle_A ; \left| \left\lfloor \frac{d}{2} \right\rfloor - 1 \right\rangle_a \right] + P [|d-1\rangle_A ; |0\rangle_a], \\ & \vdots \\ M_{1\lceil \frac{d}{2} \rceil} := & P \left[\left(|0\rangle, |1\rangle, \dots, \left| \left\lfloor \frac{d}{2} \right\rfloor \right\rangle \right)_A ; \left| \left\lfloor \frac{d}{2} \right\rfloor - 1 \right\rangle_a \right] + P \left[\left| \left\lfloor \frac{d}{2} \right\rfloor + 1 \right\rangle_A ; |0\rangle_a \right] + \dots \\ & + P \left[|d-2\rangle_A ; \left| \left\lfloor \frac{d}{2} \right\rfloor - 3 \right\rangle_a \right] + P \left[|d-1\rangle_A ; \left| \left\lfloor \frac{d}{2} \right\rfloor - 2 \right\rangle_a \right] \}. \end{aligned}$$

We analyze the branch corresponding to M_{11} ; all other outcomes M_{1m} ($m = 2, \dots, \lceil d/2 \rceil$) are treated analogously and lead to the same conclusion.

Conditioned on M_{11} , the subsets transform as follows:

$$\begin{aligned} \mathcal{A}_1^{(d, d-2k)} \rightarrow & \left\{ \left[\sum_{t=k}^{\lfloor \frac{d}{2} \rfloor - 1} \omega_{d-1-2k}^{j(t-k)} |t+1\rangle_A |00\rangle_{ab} + \omega_{d-1-2k}^{j(\lfloor \frac{d}{2} \rfloor - k)} \left| \left\lfloor \frac{d}{2} \right\rfloor + 1 \right\rangle_A |11\rangle_{ab} + \dots \right. \right. \\ & \left. \left. + \omega_{d-1-2k}^{j(d-2-2k)} |d-1-k\rangle_A \left| \left(\left\lfloor \frac{d}{2} \right\rfloor - 1 - k \right) \left(\left\lfloor \frac{d}{2} \right\rfloor - 1 - k \right) \right\rangle_{ab} \right] \left| k \circ \eta_i^{(d-2k)} \right\rangle_{\tilde{B}} \right\}, \end{aligned}$$

$$\begin{aligned}
\mathcal{A}_2^{(d,d-2k)} &\rightarrow \left\{ \left[\sum_{t=k}^{\lfloor \frac{d}{2} \rfloor - 1} \omega_{d-1-2k}^{j(t-k)} |t+1\rangle_A |00\rangle_{ab} + \omega_{d-1-2k}^{j(\lfloor \frac{d}{2} \rfloor - k)} \left| \left\langle \frac{d}{2} \right\rangle + 1 \right\rangle_A |11\rangle_{ab} + \dots \right. \right. \\
&\quad \left. \left. + \omega_{d-1-2k}^{j(d-2-2k)} |d-1-k\rangle_A \left| \left(\left\langle \frac{d}{2} \right\rangle - 1 - k \right) \left(\left\langle \frac{d}{2} \right\rangle - 1 - k \right) \right\rangle_{ab} \right] \left| \eta_i^{(d-2k)} \circ (d-1-k) \right\rangle_{\tilde{B}} \right\}, \\
\mathcal{A}_3^{(d,d-2k)} &\rightarrow \left\{ |d-1-k\rangle_A \left| \left\langle \frac{d}{2} \right\rangle - 1 - k, \left\langle \frac{d}{2} \right\rangle - 1 - k \right\rangle_{ab} \left| \xi_j^{(d-2k)} \circ \eta_i^{(d-2k)} \right\rangle_{\tilde{B}} \right\}, \\
\mathcal{B}_1^{(d,d-2k)} &\rightarrow \left\{ \left[\sum_{t=k}^{\lfloor \frac{d}{2} \rfloor} \omega_{d-1-2k}^{i(t-k)} |t\rangle_A |00\rangle_{ab} + \omega_{d-1-2k}^{i(\lfloor \frac{d}{2} \rfloor + 1 - k)} \left| \left\langle \frac{d}{2} \right\rangle + 1 \right\rangle_A |11\rangle_{ab} + \dots \right. \right. \\
&\quad \left. \left. + \omega_{d-1-2k}^{i(d-2-2k)} |d-2-k\rangle_A \left| \left(\left\langle \frac{d}{2} \right\rangle - 2 - k \right) \left(\left\langle \frac{d}{2} \right\rangle - 2 - k \right) \right\rangle_{ab} \right] \left| (d-1-k) \circ \xi_j^{(d-2k)} \right\rangle_{\tilde{B}} \right\}, \\
\mathcal{B}_2^{(d,d-2k)} &\rightarrow \left\{ \left[\sum_{t=k}^{\lfloor \frac{d}{2} \rfloor} \omega_{d-1-2k}^{i(t-k)} |t\rangle_A |00\rangle_{ab} + \omega_{d-1-2k}^{i(\lfloor \frac{d}{2} \rfloor + 1 - k)} \left| \left\langle \frac{d}{2} \right\rangle + 1 \right\rangle_A |11\rangle_{ab} + \dots \right. \right. \\
&\quad \left. \left. + \omega_{d-1-2k}^{j(d-2-2k)} |d-2-k\rangle_A \left| \left(\left\langle \frac{d}{2} \right\rangle - 2 - k \right) \left(\left\langle \frac{d}{2} \right\rangle - 2 - k \right) \right\rangle_{ab} \right] \left| \eta_i^{(d-2k)} \circ (d-1-k) \right\rangle_{\tilde{B}} \right\}, \\
\mathcal{B}_3^{(d,d-2k)} &\rightarrow \left\{ |k\rangle_A |00\rangle_{ab} \left| \eta_i^{(d-2k)} \circ \xi_j^{(d-2k)} \right\rangle_{\tilde{B}} \right\}.
\end{aligned}$$

If d is even, then additionally

$$\mathcal{A}^{(d,0)} \rightarrow \{ |\phi_r\rangle_A |\phi_s \circ \phi_t\rangle_{\tilde{B}} |00\rangle_{ab} \}.$$

Step 2 (Bob). Bob performs the POVM

$$\mathcal{M}_2 \equiv \left\{ M_{21}^0, \dots, M_{21}^{\lceil \frac{d}{2} \rceil - 2}, M_{22}^0, \dots, M_{22}^{\lceil \frac{d}{2} \rceil - 2}, M_{23}^0, \dots, M_{23}^{\lceil \frac{d}{2} \rceil - 2}, M_{24} \right\},$$

with

$$M_{24} := I_{\tilde{B}b} - \sum_{m=1}^3 \sum_{k=0}^{\lceil \frac{d}{2} \rceil - 2} M_{2m}^k,$$

and

$$\begin{aligned}
M_{21}^k &= P \left[|(|k+1\rangle, \dots, |d-1-k\rangle) \circ (|k\rangle, \dots, |d-2-k\rangle)\rangle_{\tilde{B}} ; \left| \left\langle \frac{d}{2} \right\rangle - 1 - k \right\rangle_b \right], \\
M_{22}^k &= P \left[|(d-1-k) \circ (|k+1\rangle, \dots, |d-1-k\rangle)\rangle_{\tilde{B}} ; \left(|0\rangle, |1\rangle, \dots, \left| \left\langle \frac{d}{2} \right\rangle - 2 - k \right\rangle \right)_b \right], \\
M_{23}^k &= P \left[|(|k+1\rangle, \dots, |d-1-k\rangle) \circ k\rangle_{\tilde{B}} ; \left(|0\rangle, |1\rangle, \dots, \left| \left\langle \frac{d}{2} \right\rangle - 2 - k \right\rangle \right)_b \right],
\end{aligned}$$

for $k = 0, 1, \dots, \lceil \frac{d}{2} \rceil - 2$. The outcomes corresponding to M_{21}^k , M_{22}^k , and M_{23}^k identify the subsets $\mathcal{A}_3^{(d,d-2k)}$, $\mathcal{B}_1^{(d,d-2k)}$, and $\mathcal{B}_2^{(d,d-2k)}$, respectively. If M_{24} occurs, the remaining possibilities are $\mathcal{A}_1^{(d,d-2k)}$, $\mathcal{A}_2^{(d,d-2k)}$, and $\mathcal{B}_3^{(d,d-2k)}$ (and, when d is even, also $\mathcal{A}^{(d,0)}$).

Step 3 (Alice). Alice performs

$$\mathcal{M}_3 \equiv \left\{ M_{31}^0, \dots, M_{31}^{\lceil \frac{d}{2} \rceil - 2}, M_{32} := I_{Aa} - \sum_{k=0}^{\lceil \frac{d}{2} \rceil - 2} M_{31}^k \right\},$$

where $M_{31}^k = P[|k\rangle_A; |0\rangle_a]$. If M_{31}^k clicks, the subset is $\mathcal{B}_3^{(d,d-2k)}$. Otherwise M_{32} clicks, leaving $\mathcal{A}_1^{(d,d-2k)}$ and $\mathcal{A}_2^{(d,d-2k)}$ (and, when d is even, possibly $\mathcal{A}^{(d,0)}$).

Step 4 (Bob). Bob performs

$$\mathcal{M}_4 \equiv \left\{ M_{41}^0, \dots, M_{41}^{\lceil \frac{d}{2} \rceil - 2}, M_{42}^0, \dots, M_{42}^{\lceil \frac{d}{2} \rceil - 2}, M_{43} \right\},$$

with

$$M_{43} := I_{\tilde{B}b} - \sum_{m=1}^2 \sum_{k=0}^{\lceil \frac{d}{2} \rceil - 2} M_{4m}^k,$$

and

$$\begin{aligned} M_{41}^k &= P \left[|k \circ (|k\rangle, |k+1\rangle, \dots, |d-k-2\rangle)\rangle_{\tilde{B}}; \left(|0\rangle, \dots, \left| \left\lceil \frac{d}{2} \right\rceil - 1 - k \right\rangle \right)_b \right], \\ M_{42}^k &= P \left[|(|k\rangle, |k+1\rangle, \dots, |d-k-2\rangle) \circ (d-1-k)\rangle_{\tilde{B}}; \left(|0\rangle, \dots, \left| \left\lceil \frac{d}{2} \right\rceil - 1 - k \right\rangle \right)_b \right]. \end{aligned}$$

If M_{41}^k (resp. M_{42}^k) clicks, the subset is $\mathcal{A}_1^{(d,d-2k)}$ (resp. $\mathcal{A}_2^{(d,d-2k)}$). The remaining outcome M_{43} depends on the parity of d : if d is odd, this branch is empty; if d is even, it corresponds precisely to $\mathcal{A}^{(d,0)}$.

This completes the proof for the branch M_{11} . Since the other outcomes M_{1m} lead to the same separation pattern by symmetry, the protocol perfectly identifies all subsets and hence yields perfect LOCC discrimination of \mathcal{U}_d with the stated resources. \square

Appendix B: Proof of Theorem 5

Overview and resources. We follow the resource configuration and operational idea used in Theorem 1 (teleportation plus EPR pairs used layer-by-layer). Charlie and Bob share $|\phi^+(d)\rangle_{BC}$ and Charlie teleports C to Bob, producing the bipartite state $|\psi\rangle_{A\tilde{B}}$.

Round $m = 0$ (outermost layer)

Step 1⁽⁰⁾. Alice and Bob share one EPR pair $|\phi^+(2)\rangle_{a_0b_0}$.

Step 2⁽⁰⁾ (Alice). Alice performs

$$\mathcal{M}_1^0 \equiv \{M_{11}^0, M_{12}^0\}, \quad M_{11}^0 := P[(|0\rangle, |1\rangle, \dots, |d-2\rangle)_A; |0\rangle_{a_0}] + P[|d-1\rangle_A; |1\rangle_{a_0}],$$

and $M_{12}^0 := I - M_{11}^0$. Conditioned on M_{11}^0 , the post-measurement states are exactly

$$\begin{aligned} \mathcal{A}_1^{(d,d)} &\rightarrow \left\{ \left[\left(\sum_{t=0}^{d-3} \omega_{d-1}^{jt} |t+1\rangle \right)_A |00\rangle_{a_0b_0} + \omega_{d-1}^{j(d-2)} |d-1\rangle_A |11\rangle_{a_0b_0} \right] |0 \circ \eta_i^{(d)}\rangle_{\tilde{B}} \right\}, \\ \mathcal{A}_2^{(d,d)} &\rightarrow \left\{ \left[\left(\sum_{t=0}^{d-3} \omega_{d-1}^{jt} |t+1\rangle \right)_A |00\rangle_{a_0b_0} + \omega_{d-1}^{j(d-2)} |d-1\rangle_A |11\rangle_{a_0b_0} \right] |\eta_i^{(d)} \circ (d-1)\rangle_{\tilde{B}} \right\}, \\ \mathcal{A}_3^{(d,d)} &\rightarrow \left\{ |d-1\rangle_A |11\rangle_{a_0b_0} |\xi_j^{(d)} \circ \eta_i^{(d)}\rangle_{\tilde{B}} \right\}, \\ \mathcal{B}_1^{(d,d)} &\rightarrow \left\{ |\eta_i^{(d)}\rangle_A |00\rangle_{a_0b_0} |(d-1) \circ \xi_j^{(d)}\rangle_{\tilde{B}} \right\}, \\ \mathcal{B}_2^{(d,d)} &\rightarrow \left\{ |\eta_i^{(d)}\rangle_A |00\rangle_{a_0b_0} |\xi_j^{(d)} \circ 0\rangle_{\tilde{B}} \right\}, \\ \mathcal{B}_3^{(d,d)} &\rightarrow \left\{ |0\rangle_A |00\rangle_{a_0b_0} |\eta_i^{(d)} \circ \xi_j^{(d)}\rangle_{\tilde{B}} \right\}. \end{aligned}$$

Moreover, for $k = 1, 2, \dots, \lceil \frac{d}{2} \rceil - 2$,

$$\begin{aligned}\mathcal{A}_1^{(d,d-2k)} &\rightarrow \left\{ |\xi_j^{(d-2k)}\rangle_A |00\rangle_{a_0b_0} |k \circ \eta_i^{(d-2k)}\rangle_{\tilde{B}} \right\}, \\ \mathcal{A}_2^{(d,d-2k)} &\rightarrow \left\{ |\xi_j^{(d-2k)}\rangle_A |00\rangle_{a_0b_0} |\eta_i^{(d-2k)} \circ (d-1-k)\rangle_{\tilde{B}} \right\}, \\ \mathcal{A}_3^{(d,d-2k)} &\rightarrow \left\{ |d-1-k\rangle_A |00\rangle_{a_0b_0} |\xi_j^{(d-2k)} \circ \eta_i^{(d-2k)}\rangle_{\tilde{B}} \right\}, \\ \mathcal{B}_1^{(d,d-2k)} &\rightarrow \left\{ |\eta_i^{(d-2k)}\rangle_A |00\rangle_{a_0b_0} |(d-1-k) \circ \xi_j^{(d-2k)}\rangle_{\tilde{B}} \right\}, \\ \mathcal{B}_2^{(d,d-2k)} &\rightarrow \left\{ |\eta_i^{(d-2k)}\rangle_A |00\rangle_{a_0b_0} |\xi_j^{(d-2k)} \circ k\rangle_{\tilde{B}} \right\}, \\ \mathcal{B}_3^{(d,d-2k)} &\rightarrow \left\{ |k\rangle_A |00\rangle_{a_0b_0} |\eta_i^{(d-2k)} \circ \xi_j^{(d-2k)}\rangle_{\tilde{B}} \right\}.\end{aligned}$$

If d is even, then additionally

$$\mathcal{A}^{(d,0)} \rightarrow \left\{ |\phi_r\rangle_A |\phi_s \circ \phi_t\rangle_{\tilde{B}} |00\rangle_{a_0b_0} \right\}.$$

Step 3⁽⁰⁾ (Bob). Bob performs

$$\begin{aligned}M_2^0 &\equiv \left\{ M_{21}^0 := P [| (1, \dots, d-1) \circ (0, \dots, d-2) \rangle_{\tilde{B}}; |1\rangle_{b_0} \right\}, \quad M_{22}^0 := P [| (d-1) \circ (1, \dots, d-1) \rangle_{\tilde{B}}; |0\rangle_{b_0} \right\}, \\ M_{23}^0 &:= P [| (1, \dots, d-1) \circ 0 \rangle_{\tilde{B}}; |0\rangle_{b_0} \right\}, \quad M_{24}^0 := I - M_{21}^0 - M_{22}^0 - M_{23}^0.\end{aligned}$$

Outcomes of M_{21}^0 , M_{22}^0 , M_{23}^0 identify $\mathcal{A}_3^{(d,d)}$, $\mathcal{B}_1^{(d,d)}$, and $\mathcal{B}_2^{(d,d)}$, respectively. If M_{24}^0 clicks, the remaining possibilities are $\mathcal{A}_1^{(d,d)}$, $\mathcal{A}_2^{(d,d)}$, $\mathcal{B}_3^{(d,d)}$, and all deeper-layer subsets $\mathcal{P}_l^{(d,d-2k)}$ ($\mathcal{P} = \mathcal{A}, \mathcal{B}$; $l = 1, 2, 3$; $k \geq 1$), and (when d is even) also $\mathcal{A}^{(d,0)}$.

Step 4⁽⁰⁾ (Alice). Alice performs

$$\mathcal{M}_3^0 \equiv \left\{ M_{31}^0 := P [|0\rangle_A; |0\rangle_{a_0} \right\}, \quad M_{32}^0 := I - M_{31}^0.$$

If M_{31}^0 clicks, the subset is $\mathcal{B}_3^{(d,d)}$. If M_{32}^0 clicks, the remaining subsets are $\mathcal{A}_1^{(d,d)}$, $\mathcal{A}_2^{(d,d)}$, and deeper-layer subsets (and, when d is even, possibly $\mathcal{A}^{(d,0)}$).

Step 5⁽⁰⁾ (Bob). Bob performs

$$\begin{aligned}M_4^0 &\equiv \left\{ M_{41}^0 := P [|0 \circ (0, \dots, d-2) \rangle_{\tilde{B}}; I_{b_0} \right\}, \quad M_{42}^0 := P [| (0, \dots, d-2) \circ (d-1) \rangle_{\tilde{B}}; I_{b_0} \right\}, \\ M_{43}^0 &:= I - M_{41}^0 - M_{42}^0.\end{aligned}$$

Outcomes M_{41}^0 and M_{42}^0 identify $\mathcal{A}_1^{(d,d)}$ and $\mathcal{A}_2^{(d,d)}$, respectively (and these are LOCC-distinguishable). If M_{43}^0 clicks, the remaining states lie entirely in deeper layers, and we proceed to the next round by consuming an additional EPR pair.

Iterating over inner layers

The above five-step procedure isolates the outermost layer. We then add another EPR pair $|\phi^+(2)\rangle_{a_1b_1}$ and repeat the same logic on the remaining (inner-layer) subsets. We continue this iteration until the $\lceil \frac{d}{2} \rceil - 2$ -th repetition.

Final round for odd d

If d is odd, after $\lceil \frac{d}{2} \rceil - 2 = \frac{d-3}{2}$ repetitions, the remaining subsets are exactly $\mathcal{P}_l^{(d,3)}$ ($\mathcal{P} = \mathcal{A}, \mathcal{B}$; $l = 1, 2, 3$). Let $m = \frac{d-3}{2}$. We consume the (m) -th EPR pair $|\phi^+(2)\rangle_{a_mb_m}$ and run the terminal discrimination:

Step 1^(m). Alice and Bob share $|\phi^+(2)\rangle_{a_mb_m}$.

Step 2^(m) (Alice). Alice performs

$$\mathcal{M}_1^m \equiv \left\{ M_{11}^m := P \left[\left(\left| \frac{d-3}{2} \right\rangle, \left| \frac{d-1}{2} \right\rangle \right)_A; |0\rangle_{a_m} \right] + P \left[\left| \frac{d+1}{2} \right\rangle_A; |1\rangle_{a_m} \right], \quad M_{12}^m := I - M_{11}^m \right\}.$$

Conditioned on M_{11}^m , the subsets map to the states listed in your original derivation (unchanged), namely:

$$\begin{aligned}
\mathcal{A}_1^{(d,3)} &\rightarrow \left\{ \left| \frac{d-1}{2} \right\rangle_A |00\rangle_{a_0 b_0} \dots |00\rangle_{a_m b_m} + (-1)^j \left| \frac{d+1}{2} \right\rangle_A |00\rangle_{a_0 b_0} \dots |11\rangle_{a_m b_m} \right| \left| \frac{d-3}{2} \circ \eta_i^{(3)} \right\rangle_{\tilde{B}} \right\}, \\
\mathcal{A}_2^{(d,3)} &\rightarrow \left\{ \left| \frac{d-1}{2} \right\rangle_A |00\rangle_{a_0 b_0} \dots |00\rangle_{a_m b_m} + (-1)^j \left| \frac{d+1}{2} \right\rangle_A |00\rangle_{a_0 b_0} \dots |11\rangle_{a_m b_m} \right| \left| \eta_i^{(3)} \circ \frac{d+1}{2} \right\rangle_{\tilde{B}} \right\}, \\
\mathcal{A}_3^{(d,3)} &\rightarrow \left\{ \left| \frac{d+1}{2} \right\rangle_A |00\rangle_{a_0 b_0} \dots |11\rangle_{a_m b_m} \left| \xi_j^{(3)} \circ \eta_i^{(3)} \right\rangle_{\tilde{B}} \right\}, \\
\mathcal{B}_1^{(d,3)} &\rightarrow \left\{ \left| \eta_i^{(3)} \right\rangle_A |00\rangle_{a_0 b_0} \dots |00\rangle_{a_m b_m} \left| \frac{d+1}{2} \circ \xi_j^{(3)} \right\rangle_{\tilde{B}} \right\}, \\
\mathcal{B}_2^{(d,3)} &\rightarrow \left\{ \left| \eta_i^{(3)} \right\rangle_A |00\rangle_{a_0 b_0} \dots |00\rangle_{a_m b_m} \left| \xi_j^{(3)} \circ \frac{d-3}{2} \right\rangle_{\tilde{B}} \right\}, \\
\mathcal{B}_3^{(d,3)} &\rightarrow \left\{ \left| \frac{d-3}{2} \right\rangle_A |00\rangle_{a_0 b_0} \dots |00\rangle_{a_m b_m} \left| \eta_i^{(3)} \circ \xi_j^{(3)} \right\rangle_{\tilde{B}} \right\}.
\end{aligned}$$

Step 3^(m) (Bob). Bob performs

$$\begin{aligned}
\mathcal{M}_2^m &\equiv \{ M_{21}^m := P \left[\left| \left(\frac{d-1}{2}, \frac{d+1}{2} \right) \circ \left(\frac{d-3}{2}, \frac{d-1}{2} \right) \right\rangle_{\tilde{B}} ; |1\rangle_{b_m} \right], \\
&\quad M_{22}^m := P \left[\left| \frac{d+1}{2} \circ \left(\frac{d-1}{2}, \frac{d+1}{2} \right) \right\rangle_{\tilde{B}} ; |0\rangle_{b_m} \right], \\
&\quad M_{23}^m := P \left[\left| \left(\frac{d-1}{2}, \frac{d+1}{2} \right) \circ \frac{d-3}{2} \right\rangle_{\tilde{B}} ; |0\rangle_{b_m} \right], \\
&\quad M_{24}^m := I - M_{21}^m - M_{22}^m - M_{23}^m \}.
\end{aligned}$$

Then M_{21}^m , M_{22}^m , and M_{23}^m identify $\mathcal{A}_3^{(d,3)}$, $\mathcal{B}_1^{(d,3)}$, and $\mathcal{B}_2^{(d,3)}$, respectively; M_{24}^m leaves $\mathcal{A}_1^{(d,3)}$, $\mathcal{A}_2^{(d,3)}$, and $\mathcal{B}_3^{(d,3)}$.

Step 4^(m) (Alice). Alice performs

$$\mathcal{M}_3^m \equiv \left\{ M_{31}^m := P \left[\left| \frac{d-3}{2} \right\rangle_A ; |0\rangle_{a_m} \right], M_{32}^m := I - M_{31}^m \right\}.$$

Outcome M_{31}^m identifies $\mathcal{B}_3^{(d,3)}$; otherwise M_{32}^m leaves $\mathcal{A}_1^{(d,3)}$ and $\mathcal{A}_2^{(d,3)}$.

Step 5^(m) (Bob). Bob performs

$$\mathcal{M}_4^m \equiv \left\{ M_{41}^m := P \left[\left| \frac{d-3}{2} \circ \left(\frac{d-3}{2}, \frac{d-1}{2} \right) \right\rangle_{\tilde{B}} ; I_{b_m} \right], M_{42}^m := I - M_{41}^m \right\},$$

so that M_{41}^m and M_{42}^m identify $\mathcal{A}_1^{(d,3)}$ and $\mathcal{A}_2^{(d,3)}$, respectively. Both are LOCC-distinguishable. This completes the odd- d case.

Terminal identification for even d

If d is even, after $\lceil \frac{d}{2} \rceil - 2 = \frac{d-4}{2}$ repetitions, the remaining subsets are $\mathcal{A}^{(d,0)}$ and $\mathcal{P}_l^{(d,4)}$ ($\mathcal{P} = \mathcal{A}, \mathcal{B}$; $l = 1, 2, 3$). Let $m = \frac{d-4}{2}$. The inner-layer subsets $\mathcal{A}_3^{(d,4)}$, $\mathcal{B}_1^{(d,4)}$, $\mathcal{B}_2^{(d,4)}$, and $\mathcal{B}_3^{(d,4)}$ are separated as in the odd case (with the corresponding parameters). The final discrimination step separating $\mathcal{A}_1^{(d,4)}$, $\mathcal{A}_2^{(d,4)}$, and $\mathcal{A}^{(d,0)}$ is:

Final Step (Bob). Bob performs

$$\begin{aligned}
\mathcal{M}_{\text{fin}}^m &\equiv \left\{ M_{\text{fin},1}^m := P \left[\left| \frac{d-4}{2} \circ \left(\frac{d-4}{2}, \frac{d-2}{2}, \frac{d}{2} \right) \right\rangle_{\tilde{B}} ; I_{b_m} \right], \\
&\quad M_{\text{fin},2}^m := P \left[\left| \left(\frac{d-4}{2}, \frac{d-2}{2}, \frac{d}{2} \right) \circ \frac{d+2}{2} \right\rangle_{\tilde{B}} ; I_{b_m} \right], \\
&\quad M_{\text{fin},3}^m := I - M_{\text{fin},1}^m - M_{\text{fin},2}^m \right\},
\end{aligned}$$

and the outcomes satisfy

$$M_{\text{fin},1}^m \Rightarrow \mathcal{A}_1^{(d,4)}, \quad M_{\text{fin},2}^m \Rightarrow \mathcal{A}_2^{(d,4)}, \quad M_{\text{fin},3}^m \Rightarrow \mathcal{A}^{(d,0)}.$$

Entanglement consumption. This protocol uses one teleportation round, consuming $\log_2 d$ ebits. In addition, in the m -th iteration ($m = 0, 1, \dots, \lceil \frac{d}{2} \rceil - 2$), the expected entanglement consumption between Alice and Bob is

$$\frac{(d-2m)^3 - 8 \lceil \frac{d}{2} - 1 - m \rceil}{d^3 - 8 \lceil \frac{d}{2} - 1 \rceil} \text{ ebits.}$$

Hence, the total entanglement cost is

$$\log_2 d + \sum_{m=0}^{\lceil \frac{d}{2} - 2 \rceil} \frac{(d-2m)^3 - 8 \lceil \frac{d}{2} - 1 - m \rceil}{d^3 - 8 \lceil \frac{d}{2} - 1 \rceil} \text{ ebits.}$$

Although this scheme can consume more entanglement, it is experimentally attractive because it uses only EPR pairs on top of a single teleportation round. \square

Appendix C: Proof of Theorem 6

Resources and normalization. We extend the teleportation-free idea of Theorem 2 to general d . Alice shares a maximally entangled state of local dimension $\lceil d/2 \rceil$ with Bob, and another with Charlie:

$$|\phi^+(\lceil d/2 \rceil)\rangle_{a_1 b_1} = \frac{1}{\sqrt{\lceil d/2 \rceil}} \sum_{r=0}^{\lceil d/2 \rceil - 1} |rr\rangle_{a_1 b_1}, \quad |\phi^+(\lceil d/2 \rceil)\rangle_{a_2 c_1} = \frac{1}{\sqrt{\lceil d/2 \rceil}} \sum_{r=0}^{\lceil d/2 \rceil - 1} |rr\rangle_{a_2 c_1}.$$

No teleportation is used.

Step 1 (Bob and Charlie). Bob performs the POVM

$$\mathcal{M}_1 \equiv \{M_{11}, M_{12}, \dots, M_{1\lceil d/2 \rceil}\},$$

where

$$\begin{aligned} \mathcal{M}_1 \equiv & \left\{ M_{11} := P[|0\rangle_B; |0\rangle_{b_1}] + P[|1\rangle_B; |1\rangle_{b_1}] + P\left[\left(\left|\left\lceil \frac{d}{2} \right\rceil - 1\right\rangle, \dots, |d-1\rangle\right)_B; \left|\left\lceil \frac{d}{2} \right\rceil - 1\right\rangle_{b_1}\right], \right. \\ & M_{12} := P[|0\rangle_B; |1\rangle_{b_1}] + P[|1\rangle_B; |2\rangle_{b_1}] + P\left[\left(\left|\left\lceil \frac{d}{2} \right\rceil - 1\right\rangle, \dots, |d-1\rangle\right)_B; |0\rangle_{b_1}\right], \\ & \vdots \\ & M_{1\lceil d/2 \rceil} := P\left[|0\rangle_B; \left|\left\lceil \frac{d}{2} \right\rceil - 1\right\rangle_{b_1}\right] + P[|1\rangle_B; |0\rangle_{b_1}] + P\left[\left(\left|\left\lceil \frac{d}{2} \right\rceil - 1\right\rangle, \dots, |d-1\rangle\right)_B; \left|\left\lceil \frac{d}{2} \right\rceil - 2\right\rangle_{b_1}\right] \left. \right\}. \end{aligned}$$

Charlie performs the POVM

$$\mathcal{M}_2 \equiv \{M_{21}, M_{22}, \dots, M_{2\lceil d/2 \rceil}\},$$

with elements exactly as in your original text (rewritten only for grammar/consistency):

$$\begin{aligned} \mathcal{M}_2 \equiv & \left\{ M_{21} := P\left[\left(|0\rangle, \dots, \left|\left\lceil \frac{d}{2} \right\rceil \right\rangle\right)_C; |0\rangle_{c_1}\right] + P\left[\left|\left\lceil \frac{d}{2} \right\rceil + 1\right\rangle_C; |1\rangle_{c_1}\right] + \dots + P\left[|d-1\rangle_C; \left|\left\lceil \frac{d}{2} \right\rceil - 1\right\rangle_{c_1}\right], \right. \\ & M_{22} := P\left[\left(|0\rangle, \dots, \left|\left\lceil \frac{d}{2} \right\rceil \right\rangle\right)_C; |1\rangle_{c_1}\right] + P\left[\left|\left\lceil \frac{d}{2} \right\rceil + 1\right\rangle_C; |2\rangle_{c_1}\right] + \dots + P[|d-1\rangle_C; |0\rangle_{c_1}], \\ & \vdots \\ & M_{2\lceil d/2 \rceil} := P\left[\left(|0\rangle, \dots, \left|\left\lceil \frac{d}{2} \right\rceil \right\rangle\right)_C; \left|\left\lceil \frac{d}{2} \right\rceil - 1\right\rangle_{c_1}\right] + P\left[\left|\left\lceil \frac{d}{2} \right\rceil + 1\right\rangle_C; |0\rangle_{c_1}\right] + \dots \\ & \quad \left. + P\left[|d-1\rangle_C; \left|\left\lceil \frac{d}{2} \right\rceil - 2\right\rangle_{c_1}\right] \right\}. \end{aligned}$$

We analyze the representative branch where M_{11} and M_{21} click; other branches are analogous. The corresponding post-measurement states are exactly those you listed (we keep the expressions unchanged, only standardizing punctuation and indices):

$$\begin{aligned}
\mathcal{A}_1^{(d,d-2k)} &\rightarrow \left\{ \left| \xi_j^{(d-2k)} \right\rangle_A |k\rangle_B |kk\rangle_{a_1 b_1} \left[\sum_{t=k}^{\lfloor \frac{d}{2} \rfloor} \omega_{d-1-2k}^{i(t-k)} |t\rangle_C |00\rangle_{a_2 c_1} + \dots \right. \right. \\
&\quad \left. \left. + \omega_{d-1-2k}^{i(d-2-2k)} |d-2-k\rangle_C \left| \left(\left[\frac{d}{2} \right] - 2 - k \right) \left(\left[\frac{d}{2} \right] - 2 - k \right) \right\rangle_{a_2 c_1} \right] \right\}, \\
\mathcal{A}_2^{(d,d-2k)} &\rightarrow \left\{ \left| \xi_j^{(d-2m)} \right\rangle_A \left[|k\rangle_B |kk\rangle_{a_1 b_1} + \dots + \sum_{t=\lceil \frac{d}{2} \rceil - 1}^{d-2-k} \omega_{d-1-2k}^{i(t-k)} |t\rangle_B \left| \left(\left[\frac{d}{2} \right] - 1 \right) \left(\left[\frac{d}{2} \right] - 1 \right) \right\rangle_{a_1 b_1} \right] \right. \\
&\quad \left. |d-1-k\rangle_C \left| \left(\left[\frac{d}{2} \right] - 1 - k \right) \left(\left[\frac{d}{2} \right] - 1 - k \right) \right\rangle_{a_2 c_1} \right\}, \\
\mathcal{A}_3^{(d,d-2k)} &\rightarrow \left\{ |d-1-k\rangle_A \left[|k+1\rangle_B |(k+1)(k+1)\rangle_{a_1 b_1} + \dots + \sum_{t=\lceil \frac{d}{2} \rceil - 2}^{d-2-k} \omega_{d-1-2k}^{j(t-k)} |t+1\rangle_B \right. \right. \\
&\quad \left. \left| \left(\left[\frac{d}{2} \right] - 1 \right) \left(\left[\frac{d}{2} \right] - 1 \right) \right\rangle_{a_1 b_1} \right] \left[\sum_{t=k}^{\lfloor \frac{d}{2} \rfloor} \omega_{d-1-2m}^{i(t-m)} |t\rangle_C |00\rangle_{a_2 c_1} + \dots \right. \\
&\quad \left. \left. + \omega_{d-1-2k}^{i(d-2-2k)} |d-2-k\rangle_C \left| \left(\left[\frac{d}{2} \right] - 2 - k \right) \left(\left[\frac{d}{2} \right] - 2 - k \right) \right\rangle_{a_2 c_1} \right] \right\}, \\
\mathcal{B}_1^{(d,d-2k)} &\rightarrow \left\{ \left| \eta_i^{(d-2k)} \right\rangle_A |d-1-k\rangle_B \left| \left(\left[\frac{d}{2} \right] - 1 \right) \left(\left[\frac{d}{2} \right] - 1 \right) \right\rangle_{a_1 b_1} \left[\sum_{t=k}^{\lfloor \frac{d}{2} \rfloor - 1} \omega_{d-1-2k}^{j(t-k)} |t+1\rangle_C \right. \right. \\
&\quad \left. \left. |00\rangle_{a_2 c_1} + \dots + \omega_{d-1-2k}^{j(d-2-2k)} |d-1-k\rangle_C \left| \left(\left[\frac{d}{2} \right] - 1 - k \right) \left(\left[\frac{d}{2} \right] - 1 - k \right) \right\rangle_{a_2 c_1} \right] \right\}, \\
\mathcal{B}_2^{(d,d-2k)} &\rightarrow \left\{ \left| \eta_i^{(d-2k)} \right\rangle_A \left[|k+1\rangle_B |(k+1)(k+1)\rangle_{a_1 b_1} + \dots + \sum_{t=\lceil \frac{d}{2} \rceil - 2}^{d-2-k} \omega_{d-1-2k}^{j(t-k)} |t+1\rangle_B \right. \right. \\
&\quad \left. \left| \left(\left[\frac{d}{2} \right] - 1 \right) \left(\left[\frac{d}{2} \right] - 1 \right) \right\rangle_{a_1 b_1} \right] |k\rangle_C |00\rangle_{a_2 c_1} \right\}, \\
\mathcal{B}_3^{(d,d-2k)} &\rightarrow \left\{ |k\rangle_A \left[|k\rangle_B |kk\rangle_{a_1 b_1} + \dots + \sum_{t=\lceil \frac{d}{2} \rceil - 1}^{d-2-k} \omega_{d-1-2k}^{i(t-k)} |t\rangle_B \left| \left(\left[\frac{d}{2} \right] - 1 \right) \left(\left[\frac{d}{2} \right] - 1 \right) \right\rangle_{a_1 b_1} \right] \right. \\
&\quad \left. \left[\sum_{t=k}^{\lfloor \frac{d}{2} \rfloor - 1} \omega_{d-1-2k}^{j(t-k)} |t+1\rangle_C |00\rangle_{a_2 c_1} + \dots + \omega_{d-1-2k}^{j(d-2-2k)} |d-1-k\rangle_C \right. \right. \\
&\quad \left. \left. \left| \left(\left[\frac{d}{2} \right] - 1 - k \right) \left(\left[\frac{d}{2} \right] - 1 - k \right) \right\rangle_{a_2 c_1} \right] \right\}.
\end{aligned}$$

If d is even, then additionally

$$\mathcal{A}^{(d,0)} \rightarrow \left\{ |\phi_r\rangle_A |\phi_s\rangle_B |\phi_t\rangle_C \left| \left(\left[\frac{d}{2} \right] - 1 \right) \left(\left[\frac{d}{2} \right] - 1 \right) \right\rangle_{a_1 b_1} |00\rangle_{a_2 c_1} \right\}.$$

Step 2 (Alice). Alice performs the POVM \mathcal{M}_3 defined by

$$\mathcal{M}_3 \equiv \left\{ M_{31}^0, \dots, M_{31}^{\lceil \frac{d}{2} \rceil - 2}, M_{32}^0, \dots, M_{32}^{\lceil \frac{d}{2} \rceil - 2}, M_{33} \right\},$$

where

$$M_{33} = I - \sum_{m=1}^2 \sum_{k=0}^{\lceil \frac{d}{2} \rceil - 2} M_{3m}^k,$$

and

$$\begin{aligned} M_{31}^k &:= P \left[(|k+1\rangle, \dots, |d-1-k\rangle)_A; |k\rangle_{a_1}; \left(|0\rangle, \dots, \left| \left\lceil \frac{d}{2} \right\rceil - 2 - k \right\rangle \right)_{a_2} \right], \\ M_{32}^k &:= P \left[|d-1-k\rangle_A; \left(|k+1\rangle, \dots, \left| \left\lceil \frac{d}{2} \right\rceil - 1 \right\rangle \right)_{a_1}; \left(|0\rangle, \dots, \left| \left\lceil \frac{d}{2} \right\rceil - 2 - k \right\rangle \right)_{a_2} \right]. \end{aligned}$$

These outcomes identify

$$M_{31}^k \Rightarrow \mathcal{A}_1^{(d,d-2k)}, \quad M_{32}^k \Rightarrow \mathcal{A}_3^{(d,d-2k)},$$

while M_{33} leaves $\mathcal{A}_2^{(d,d-2k)}$ or $\mathcal{B}_l^{(d,d-2k)}$ ($l = 1, 2, 3$) (and, if d is even, possibly also $\mathcal{A}^{(d,0)}$). We proceed with the M_{33} branch.

Step 3 (Charlie). Charlie performs

$$\mathcal{M}_4 \equiv \left\{ M_{41}^0, \dots, M_{41}^{\lceil \frac{d}{2} \rceil - 2}, M_{42} \right\}, \quad M_{42} = I - \sum_{k=0}^{\lceil \frac{d}{2} \rceil - 2} M_{41}^k,$$

where $M_{41}^k := P[|k\rangle_C; |0\rangle_{c_1}]$. If M_{41}^k clicks, the subset is $\mathcal{B}_2^{(d,d-2k)}$. Otherwise (M_{42}), the remaining subsets are $\mathcal{A}_2^{(d,d-2k)}$, $\mathcal{B}_1^{(d,d-2k)}$, and $\mathcal{B}_3^{(d,d-2k)}$ (and, when d is even, possibly $\mathcal{A}^{(d,0)}$).

Step 4 (Bob). Bob performs

$$\mathcal{M}_5 \equiv \left\{ M_{51}^0, \dots, M_{51}^{\lceil \frac{d}{2} \rceil - 2}, M_{52} \right\}, \quad M_{52} = I - \sum_{k=0}^{\lceil \frac{d}{2} \rceil - 2} M_{51}^k,$$

where

$$M_{51}^k := P \left[|d-1-k\rangle_B; \left| \left\lceil \frac{d}{2} \right\rceil - 1 \right\rangle_{b_1} \right].$$

If M_{51}^k clicks, the subset is $\mathcal{B}_1^{(d,d-2k)}$; otherwise, the remaining subsets are $\mathcal{A}_2^{(d,d-2k)}$ and $\mathcal{B}_3^{(d,d-2k)}$ (and, when d is even, possibly $\mathcal{A}^{(d,0)}$).

Step 5 (Alice). Finally, Alice performs

$$\mathcal{M}_6 \equiv \left\{ M_{61}^0, \dots, M_{61}^{\lceil \frac{d}{2} \rceil - 2}, M_{62}^0, \dots, M_{62}^{\lceil \frac{d}{2} \rceil - 2}, M_{63} \right\},$$

where

$$M_{63} = I - \sum_{m=1}^2 \sum_{k=0}^{\lceil \frac{d}{2} \rceil - 2} M_{6m}^k,$$

and

$$\begin{aligned} M_{61}^k &:= P \left[(|k+1\rangle, \dots, |d-1-k\rangle)_A; \left(|k\rangle, \dots, \left| \left\lceil \frac{d}{2} \right\rceil - 1 \right\rangle \right)_{a_1}; \left| \left\lceil \frac{d}{2} \right\rceil - 1 - k \right\rangle_{a_2} \right], \\ M_{62}^k &:= P \left[|k\rangle_A; \left(|k\rangle, \dots, \left| \left\lceil \frac{d}{2} \right\rceil - 1 \right\rangle \right)_{a_1}; \left(|0\rangle, \dots, \left| \left\lceil \frac{d}{2} \right\rceil - 1 - k \right\rangle \right)_{a_2} \right]. \end{aligned}$$

Outcomes M_{61}^k and M_{62}^k identify $\mathcal{A}_2^{(d,d-2k)}$ and $\mathcal{B}_3^{(d,d-2k)}$, respectively. The remaining outcome M_{63} depends on the parity of d : if d is odd, this branch is empty; if d is even, it corresponds exactly to $\mathcal{A}^{(d,0)}$.

Conclusion and resource cost. All subsets in \mathcal{U}_d in Eq. (4) are deterministically identified without teleportation. The total entanglement consumption is therefore

$$2 \log_2(\lceil d/2 \rceil) \text{ ebits},$$

as stated in Theorem 6. \square

[1] T. Eggeling and R. F. Werner, Hiding classical data in multipartite quantum states, *Phys. Rev. Lett.* **89**, 097905 (2002).

[2] D. P. DiVincenzo, D. W. Leung, and B. M. Terhal, Quantum data hiding, *IEEE Trans. Inf. Theory* **48**, 580 (2002).

[3] W. Matthews, S. Wehner and A. Winter, Distinguishability of quantum states under restricted families of measurements with an application to quantum data hiding, *Commun. Math. Phys.* **291**, 813–843 (2009).

[4] G. P. Guo, C. F. Li, B. S. Shi, J. Li, and G. C. Guo, Quantum key distribution scheme with orthogonal product states, *Phys. Rev. A* **64**, 042301 (2001).

[5] H. K. Lo and H. F. Chau, Unconditional security of quantum key distribution over arbitrarily long distances, *Science* **283**, 2050–2056 (1999).

[6] L. Y. Hsu and C. M. Li, Quantum secret sharing using product states, *Phys. Rev. A* **71**, 022321 (2005).

[7] J. Wang, L. Li, H. Peng, and Y. Yang, Quantum-secret-sharing scheme based on local distinguishability of orthogonal multi-qudit entangled states, *Phys. Rev. A* **95**, 022320 (2017).

[8] R. Rahaman and M. G. Parker, Quantum scheme for secret sharing based on local distinguishability, *Phys. Rev. A* **91**, 022330 (2015).

[9] D. Markham and B. C. Sanders, Graph states for quantum secret sharing, *Phys. Rev. A* **78**, 042309 (2008).

[10] C. H. Bennett *et al.*, Quantum nonlocality without entanglement, *Phys. Rev. A* **59**, 1070 (1999).

[11] C. H. Bennett *et al.*, Unextendible product bases and bound entanglement, *Phys. Rev. Lett.* **82**, 5385 (1999).

[12] D. P. DiVincenzo *et al.*, Unextendible product bases, uncompletable product bases and bound entanglement, *Commun. Math. Phys.* **238**, 379–410 (2003).

[13] S. D. Rinaldis, Distinguishability of complete and unextendible product bases, *Phys. Rev. A* **70**, 022309 (2004).

[14] S. Ghosh *et al.*, Distinguishability of Bell states, *Phys. Rev. Lett.* **87**, 277902 (2001).

[15] Y. Feng and Y. Y. Shi, Characterizing locally indistinguishable orthogonal product states, *IEEE Trans. Inf. Theory* **55**, 2799–2806 (2009).

[16] Y. H. Yang *et al.*, Characterizing unextendible product bases in multi-qudit system, *Sci. Rep.* **5**, 11963 (2015).

[17] S. Halder, Several nonlocal sets of multipartite orthogonal product states, *Phys. Rev. A* **98**, 022303 (2018).

[18] G. B. Xu *et al.*, Quantum nonlocality of multipartite orthogonal product states, *Phys. Rev. A* **93**, 032341 (2016).

[19] Y. L. Wang *et al.*, The local indistinguishability of multipartite product states, *Quantum Inf. Process.* **16**, 5 (2017).

[20] Z. C. Zhang *et al.*, Construction of nonlocal multipartite quantum states, *Phys. Rev. A* **95**, 052344 (2017).

[21] J. Walgate and L. Hardy, Nonlocality, asymmetry, and distinguishing bipartite states, *Phys. Rev. Lett.* **89**, 147901 (2002).

[22] H. Q. Zhou, T. Gao, and F. L. Yan, Orthogonal product sets with strong quantum nonlocality on a plane structure, *Phys. Rev. A* **106**, 052209 (2022).

[23] H. Q. Zhou, T. Gao, and F. L. Yan, Strong quantum nonlocality without entanglement in an n -partite system with even n , *Phys. Rev. A* **107**, 042214 (2023).

[24] H. Q. Zhou, T. Gao, and F. L. Yan, Strong quantum nonlocality without entanglement in every $(n-1)$ -partition, *iScience* **28**, 111528 (2025).

[25] M. Y. Hu, T. Gao, and F. L. Yan, Strong quantum nonlocality with genuine entanglement in an N -qutrit system, *Phys. Rev. A* **109**, 022220 (2024).

[26] M. Y. Hu, T. Gao, and F. L. Yan, Strongest quantum nonlocality in N -partite systems, *Phys. Rev. A* **112**, 032205 (2025).

[27] Y. L. Wang *et al.*, Nonlocality of orthogonal product-basis quantum states, *Phys. Rev. A* **92**, 032313 (2015).

[28] J. Niset and N. J. Cerf, Multipartite nonlocality without entanglement in many dimensions, *Phys. Rev. A* **74**, 052103 (2006).

[29] P. Yuan, G. J. Tian, and X. M. Sun, Strong quantum nonlocality without entanglement in multipartite quantum systems, *Phys. Rev. A* **102**, 042228 (2020).

[30] Y. Y. He, F. Shi, and X. D. Zhang, Strong quantum nonlocality and unextendibility without entanglement in N -partite systems with odd N , *Quantum* **8**, 1349 (2024).

[31] D. H. Jiang and G. B. Xu, Nonlocal sets of orthogonal product states in an arbitrary multipartite quantum system, *Phys. Rev. A* **102**, 032211 (2020).

[32] Z. C. Zhang *et al.*, Nonlocality of orthogonal product states, *Phys. Rev. A* **92**, 012332 (2015).

[33] S. Croke and S. M. Barnett, Difficulty of distinguishing product states locally, *Phys. Rev. A* **95**, 012337 (2017).

[34] S. Halder *et al.*, Strong quantum nonlocality without entanglement, *Phys. Rev. Lett.* **122**, 040403 (2019).

[35] M. S. Li and Z. J. Zheng, Genuine hidden nonlocality without entanglement: from the perspective of local discrimination, *New J. Phys.* **24**, 043036 (2022).

[36] F. Shi *et al.*, Unextendible product bases from tile structures and their local entanglement-assisted distinguishability, *Phys. Rev. A* **101**, 062329 (2020).

[37] F. Shi *et al.*, Strongly nonlocal unextendible product bases do exist, *Quantum* **6**, 619 (2022).

[38] S. M. Cohen, Local approximation for perfect discrimination of quantum states, *Phys. Rev. A* **107**, 012401 (2023).

[39] Z. C. Zhang, X. Wu, and X. Zhang, Locally distinguishing unextendible product bases by using entanglement efficiently, *Phys. Rev. A* **101**, 022306 (2020).

- [40] S. Bandyopadhyay, S. Halder, and M. Nathanson, Optimal resource states for local state discrimination, *Phys. Rev. A* **97**, 022314 (2018).
- [41] S. M. Cohen, Local distinguishability with preservation of entanglement, *Phys. Rev. A* **75**, 052313 (2007).
- [42] S. Rout *et al.*, Genuinely nonlocal product bases: classification and entanglement-assisted discrimination, *Phys. Rev. A* **100**, 032321 (2019).
- [43] S. M. Cohen, Understanding entanglement as resource: locally distinguishing unextendible product bases, *Phys. Rev. A* **77**, 012304 (2008).
- [44] Z. C. Zhang *et al.*, Local distinguishability of orthogonal quantum states with multiple copies of $2 \otimes 2$ maximally entangled states, *Phys. Rev. A* **97**, 022334 (2018).
- [45] Y. X. Yan *et al.*, Variational LOCC-assisted quantum circuits for long-range entangled states, *Phys. Rev. Lett.* **134**, 170601 (2025).
- [46] R. Horodecki *et al.*, Quantum entanglement, *Rev. Mod. Phys.* **81**, 865 (2009).
- [47] T. Gao, F. L. Yan, and S. J. van Enk, Permutationally invariant part of a density matrix and nonseparability of N -qubit states, *Phys. Rev. Lett.* **112**, 180501 (2014).
- [48] T. Gao and Y. Hong, Detection of genuinely entangled and nonseparable n -partite quantum states, *Phys. Rev. A* **82**, 062113 (2010).
- [49] F. L. Yan, T. Gao, and E. Chitambar, Two local observables are sufficient to characterize maximally entangled states of N qubits, *Phys. Rev. A* **83**, 022319 (2011).
- [50] S. Morelli, M. Huber, and A. Tavakoli, Resource-efficient high-dimensional entanglement detection via symmetric projections, *Phys. Rev. Lett.* **131**, 170201 (2023).
- [51] F. F. Du, X. M. Ren, and J. Guo, Error-heralded high-dimensional quantum gate with robust fidelity, *Optics Express* **32**, 31633 (2024).